Journal of Visualization, Vol. 10, No. 1 (2007)11-16

Review Report

Heat Flux Sensors and Infrared Thermography

Carlomagno, G. M.*

* Università di Napoli "Federico II", DETEC, Piazzale Tecchio 80, 80125 Napoli, Italy.
E-mail: carmagno@unina.it

Received 29 November 2006

1. Introduction

Measuring convective heat flux rates over a surface is a difficult task and generally requires a sensor (with its specific thermal model) and a temperature transducer (Thompson, 1981). If temperature is measured by thermocouples or resistance temperature detectors (RTD), each transducer yields either the heat flux at a given point, or the space-averaged one. Hence, in terms of spatial resolution, the transducer can be considered as *zero-dimensional*. This behavior makes measuring particularly laborious whenever temperature, and/or heat flux, fields exhibit spatial variations.

An optical access to the exchanging surface in the employed band existing, the Infrared Scanning Radiometer (IRSR) becomes a true two-dimensional temperature transducer since it may perform accurate measurement of surface temperature maps even if rather high gradients exist. As a consequence, the heat flux sensor becomes two-dimensional as well. In this case, *infrared thermography* (IRT), as it is called the use of IRSR, can be exploited to measure convective heat fluxes, in both steady and transient techniques (Carlomagno, 1997), (Carlomagno et al., 2001). Thermal maps produced by modern computerized thermographic systems are composed of a large amount of pixels ($40k$ to $300k$) that can be obtained with a response time down to $10^{-3}s$.

Exploitation of IRSR to perform heat transfer measurement is very convenient from many points of view as compared to standard transducers. Indeed, IRSR is fully two-dimensional so it can analyze the thermal effects of complex fluid flows, it allows the evaluation of errors due to tangential conduction, as well to radiation, it has a low response time and it is non-intrusive. E.g., this allows avoiding conduction errors through thermocouple, or RTD, wires.

This paper describes the use of some sensors with IRT to measure wall convective heat fluxes. The most used sensors are critically reviewed and their different operating methods, together with the necessary implementations, are discussed. Finally, some applications are presented.

2. Heat Flux Sensors

Heat flux sensors consist of slabs with a known thermal behavior, whose temperature is to be measured at given points. The energy conservation equation applied to the sensor model yields the relationship that correlates measured temperature to heat transfer rate. Most of the used sensors are the *one-dimensional* ones, where heat flux is assumed to be normal to the sensing surface.

The usually adopted heat flux sensor models are:

1. **Thin-film.** A very thin resistance thermometer (*film*) measures in a transient mode the surface temperature of a *thermally thicker* slab to which is bonded. Heat flux rate is inferred from the theory of *heat conduction in a semi-infinite wall*. To use this sensor, the heat exchanging surface must be necessarily viewed by IRSR.
2. **Thick-film.** The slab is used as a calorimeter, heat flux being obtained in a transient mode from the *time rate of change of the mean slab temperature*. This temperature is measured by using the slab as a resistance thermometer and cannot be monitored by IRSR.
3. **Thin-skin.** The slab is *thermally thin* (i.e., temperature may be assumed constant across its thickness) and, as for the thick-film sensor, is again used as a calorimeter. Heat flux rate is inferred in a transient mode from the *time rate of change of the slab temperature*. Either one of the slab surfaces can be generally used for measuring purposes.
4. **Gradient.** By considering a *steady state* heat transfer process, heat flux rate is computed by measuring the *temperature difference across the slab*. This temperature difference is usually

measured by thermopiles made of very thin thermocouples, or by *thin-film* thermometers. To author's knowledge, this sensor has never been used with infrared thermography.

5. **Heated-thin-foil.** The sensor consists of steadily heating a *thermally thin* metallic foil, or a printed circuit board, by Joule effect, the heat flux rate being measured from an overall energy balance. Due the foil thermal thinness, also in this sensor either one of the slab surfaces can be generally viewed by IRSR. The use of this sensor involves a steady technique.

Application of IRSR to the *thick-film* and *gradient* sensors is either not possible, or not very practical, therefore, the *thin-film* and the *thin-skin* sensors, regarding transient techniques, together with the *heated-thin-foil* sensor, regarding a steady technique, will be treated in the following.

For the ***thin-film***, the heat-flux sensor will be anyhow constituted by a slab of finite thickness *s*; hence, the *thin-film* model will be applicable only for rather small measuring times. On quantitative basis, if t_M is the effective measuring time, the following condition has to be satisfied:

$$t_M < \frac{s^2}{2\alpha} \tag{1}$$

where α is the slab thermal diffusivity coefficient. Therefore, for this sensor the boundary condition on the back surface is irrelevant as long as the assumption of semi-infinite wall is valid.

By assuming the sensor to be initially ($t = 0$) isothermal at temperature $T_i = T_w(0)$, a suitable formula to evaluate the heat flux from the measured sensor surface temperature T_w is:

$$Q_c - Q_r = \sqrt{\frac{\rho c \lambda}{\pi}} \left[\frac{\phi\,(t)}{\sqrt{t}} + \frac{1}{2} \int_0^t \frac{\phi\,(t) - \phi\,(\xi)}{(t-\xi)^{3/2}} d\xi \right] \tag{2}$$

where: Q_r is the radiative heat flux to ambient; Q_c is the convective heat flux; $\phi = T_w(t) - T_{wi}$; ρ, c and λ, are mass density, specific heat and thermal conductivity coefficient of sensor material, respectively.

The radiative heat flux can be evaluated as:

$$Q_r = \sigma\varepsilon\left(T_w^4 - T_{amb}^4\right) \tag{3}$$

where: σ is the Stefan-Boltzmann constant; ε is the total emissivity coefficient; T_{amb} is the average ambient temperature.

The convective heat flux can be expressed according to the generalized Newton law:

$$Q_c = h\,(T_w - T_r) \tag{4}$$

where h is the convective heat transfer coefficient and T_r is a reference temperature. This one mainly depends on the stream fluid dynamic conditions; for high Mach number (or mixing of streams at different temperatures), the correct choice is the *adiabatic wall temperature* T_{aw} (Meola et al., 1996), while, for low speed flows, the reference temperature coincides with the free stream one.

The integral of Eq.(2) can be numerically evaluated by using one of the algorithms generally accepted in aerospace (Cook et al., 1996). However, these algorithms are generally sensitive to errors in temperature measurement, to noisy data and to inexact knowledge of the starting time. Besides, the approach based on Eq.(2) needs a high data sampling rate which, for fast transients, cannot be satisfied by *standard* IRSR's which have an acquisition frequency of 50 or 60*Hz*.

To bypass this problem, another way is based on the assumption that the flow yields a certain heat flux time variation law with some free parameters and such parameters are found so that computed temperatures best agree with the experimentally measured ones (de Luca et al., 1995). E.g., the best fit may be determined by means of the ordinary least squares criterion.

In fact, for a constant h and constant reference temperature T_r, the solution of the heat diffusion equation, obtained by means of Laplace transforms, gives for the surface temperature:

$$T_w = T_{wi} + (T_r - T_{wi})\left(1 - e^{\beta^2} erfc\beta\right) \quad ; \quad \beta = h\sqrt{t}/\sqrt{\rho c\lambda} \tag{5}$$

In the presence of a radiative heat flux and under the assumption that the convection and radiation are uncoupled, Eq.(5) can be modified to take into account also the radiative contribute:

$$T_w = T_{wi} + (T_r - T_{wi})\left(1 - e^{\beta^2} erfc(\beta)\right) - \frac{Q_r}{h} \tag{6}$$

The ***thin-skin*** sensor, practically an isothermal plate, is modeled as an ideal calorimeter, heated on one surface and thermically insulated at the other one. The unsteady energy balance gives:

$$Q_c + Q_r = \rho\, cs\, \frac{dT_w}{dt} \tag{7}$$

where: T_w is the only local sensor temperature; ρ, c and s, are mass density, specific heat and thickness of sensor material, respectively.

Then, from Eq.(4) and by knowing the temperature evolution, the convective heat transfer coefficient can be evaluated. If the slab surface not contacting the flow is not thermically insulated, Eq.(7) must be implemented to include the total heat flux to external ambient Q_a which consists of the sum of radiative and natural convection fluxes. The radiative part can be again evaluated with (2), while natural convection can be computed with literature data (e.g., Kakac et al., 1987).

As already mentioned, for both *thin-skin* and *thin-film* models, the heat flux within the sensor is assumed to be one-dimensional. This hypothesis is only satisfied when sensor surface temperature is constant. However, in complex flows, temperature may vary along the surface, so that tangential conduction within the sensor occurs. If sensor material is isotropic, one can split conduction effects in the two tangential directions and, by assuming a harmonically varying flux, the problem is solved for both sensors (Carlomagno, 1997), the extension to any other heat flux being straightforward. Thus, each temperature harmonic component may be corrected and the corresponding heat flux component can be evaluated by using the one-dimensional formulae.

A method, having a very effective application of IRSR, is the steady state ***heated-thin-foil*** technique. The sensor, made of a thin metallic foil or a printed circuit board, is heated by Joule effect. In the following, the sensor is again initially supposed one-dimensional and the surface not exposed to flow, adiabatic. By making a one-dimensional steady state local energy balance, it is found:

$$Q_j = Q_r + Q_c \tag{8}$$

where Q_j is the imposed constant Joule heat flux.

From Eqs.(2), (3) and (8), the explicit expression for h is:

$$h = \frac{Q_j - \sigma\varepsilon\left(T_w^4 - T_{amb}^4\right)}{T_w - T_r} \tag{9}$$

By assuming a small Biot number $Bi = hs/\lambda$ (s and λ are the thickness and thermal conductivity coefficient of the foil, respectively) as compared to unity, temperature is constant across foil thickness, so the foil surface to be measured can also be that opposite to the heat exchanging surface. If the surface not contacting the flow is not fully adiabatic, Eq.(9) must be implemented to include the total heat flux to external ambient Q_a as suggested before for the *thin-skin* sensor, or by making some *ad hoc* tests after insulating the surface which is exchanging heat with fluid.

Also the *heated-thin-foil* technique can be used when heat transfer involves surface temperature gradients that cause tangential conduction which constitute a relevant percentage of the measured flux. By retaining the assumption of thermally thin sensor, it is possible to evaluate (for an isotropic slab) the mean tangential conduction flux Q_k simply by means of Fourier law:

$$Q_k = -\lambda s \nabla^2 T_w \tag{10}$$

By including tangential conduction, the convective heat transfer coefficient becomes:

$$h = \frac{Q_j - \sigma\varepsilon\left(T_w^4 - T_{amb}^4\right) - Q_a + Q_k}{T_w - T_r} \tag{11}$$

It is important to evidence that IRSR (intrinsically two-dimensional) certainly enables to evaluate the Laplacian of Eq.(10) by numerical computation. However, this can be performed only after an adequate filtering of the radiometer signal which is typically affected by noise.

In many applications of the *heated-thin-foil* sensor, a spatially constant heating can be easily obtained by using a printed circuit board (Astarita, 1996). This one can be made with several adjacent thin (down to 5μm) copper tracks arranged in a Greek fret mode and bound to a fibreglass substrate. Due to the copper high conductivity coefficient, the board exhibits an anisotropic thermal conduction behavior so the conductive heat flux cannot be evaluated with Eq.(10).

By still retaining the assumption that T_w is independent of the coordinate normal to the slab, it is therefore necessary to generalize Eq.(10) so as to take into account this anisotropy:

$$Q_k(x,y) = -\underline{\nabla} \cdot \left(s(x,y)\underline{\underline{\Lambda}}(x,y) \cdot \underline{\nabla} T_w(x,y) \right) \tag{12}$$

where $\underline{\underline{\Lambda}}$ is the thermal conductivity tensor. In the case of a Greek fret printed circuit board, to simplify Eq.(12), it is possible to substantially separate the effect due to the copper tracks from that of the fibreglass support (Astarita, 1996) and easily solve the problem.

3. Applications

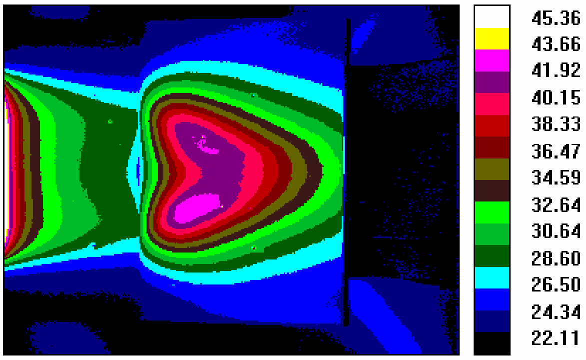

Fig. 1. Flat Plate with Ramp in Hypersonic Flow at M = 6.

In order to show the capability of IRSR to measure heat transfer in complex fluid flows, in this section some examples of its exploitation are reported.

Knowledge of thermal loads on surfaces exposed to hypersonic flows is essential for the effective design of thermal protection systems.

Figure 1 shows the thermal map, recorded in the HEAT Centrospazio (Pisa) tunnel, for a two-dimensional hypersonic flow over a flat plate followed by a 15° compression ramp (wedge), with its hinge line parallel to the plate leading edge. Flow is from left to right and. Mach number M = 6. The model surface (*thin-film*) is made of two MACOR™ (low thermal conductivity) plates.

The thermal map, recorded about 80*ms* after flow starting, clearly shows the potential conical core downstream of tunnel exit and the initial continuous decrease of the wall temperature, due to boundary layer development. Near the hinge line, is distinctly visible a zone where temperature attains a minimum which is due to existence, there, of a flow separation region. Continuing to move along the symmetry axis and after the hinge line, the temperature reaches a maximum which is due to flow reattachment on the inclined ramp. Results well agree with literature data.

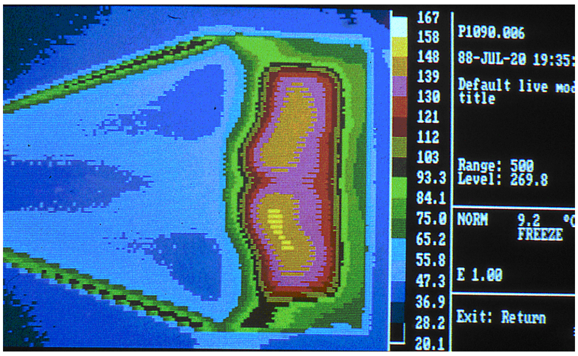

Fig. 2. Delta Wing with Ramp in Hypersonic Flow at M = 8.15.

A delta (swept angle 70°) wing with ramp (ramp angle 15°) is tested by injecting it in the H210 CEAT (Poitiers) hypersonic tunnel at zero incidence and M = 8.15. Its surface is made of a 0.5*mm* thick SS plate (*thin-skin*). The thermal map of Fig. 2, taken 1.8*s* after injection, is dated (1988), so stripes between two interlaced fields (0.08*s* apart) are visible and the wing surface shows almost isothermal because of the low IRSR dynamic range (8 bits). However, separation and flow reattachment are still clearly visible.

The adiabatic wall temperature T_{aw}, already mentioned in section 3, can be measured by means of a thin (to avoid tangential conduction) foil, provided heat flux from the surface non contacting the flow is negligible. Practically, this means using a *non-heated-thin-foil* technique, or a *thin-skin* one at steady state.

Figure 3 shows the map of T_{aw} for a jet, issuing from a 5 *mm* nozzle at M = 0.85 and impinging on a plate (made with a 50 *μm* thick SS foil) at a distance z = 20 *mm*. The thermal map is non axisymmetric and shows the instability that is found in jets for Mach number greater than 0.7. In this case it has to be evidenced the simplicity with which is possible to measure the detailed adiabatic wall temperature distribution, as that reported in Fig. 3, just by using a non heated thin foil.

The spiral vortices, arising in the transitional regime of the three-dimensional boundary layer on a rotating disk (*which are rotating attached to the disk surface*) are detected by heating the disk surface with a printed circuit board (*heated-thin-foil*) and by using the line scan mode of IRSR to measure radial temperature profiles. Due to disk rotation, each acquired line is displaced, relative to the disk surface, of an angle that is function of rotating speed and acquisition frequency. So, a numerical reconstruction of the thermal image (Astarita et al., 2002) can be performed with several thousands profiles as shown in Fig. 4, the disk Reynolds number being *Re* = 310,000 and disk diameter 450 *mm.*

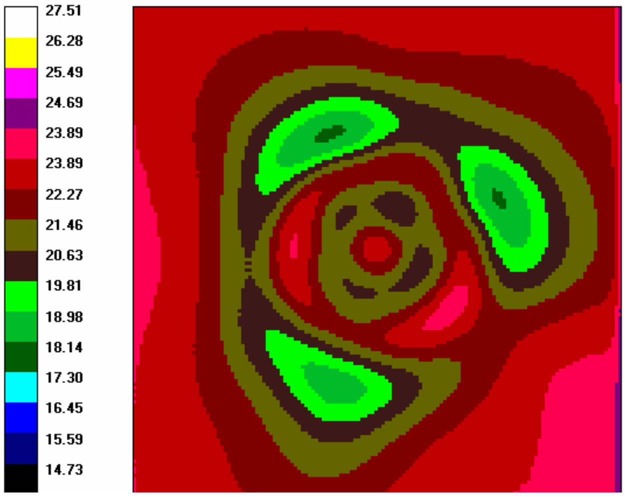

Fig. 3. T_{aw} for z/D = 4, M = 0.85.

In order to understand the thermal map, it has to be noticed that, due to the constant imposed heat flux, increasing the convective heat transfer coefficient, and/or decreasing air temperature, decreases the disk temperature and this explains the wall temperature variations towards the disk edge. In fact, each vortex takes fresh air from ambient pushing it towards the disk surface and so producing a decrease of the surface temperature. This latter one is also due to the impinging jet effect, induced by the vortex, which increases at the same location the convective heat transfer coefficient. Besides, the air flowing over the disk surface increases its bulk temperature by increasing wall temperature. Both, these effects cause the surface temperature variations at the disk edge.

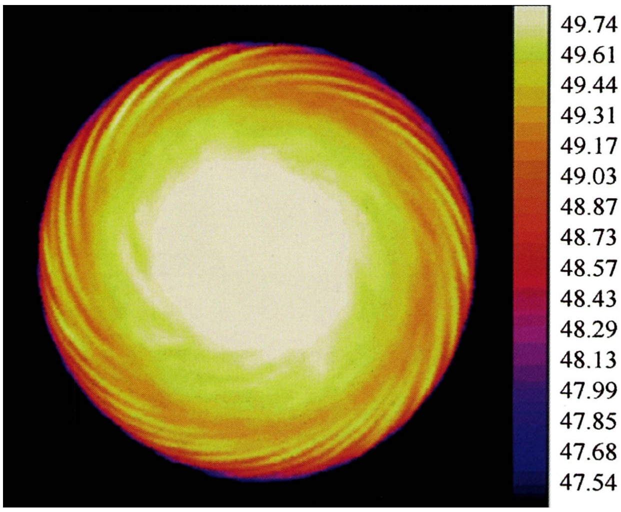

Fig. 4. Spiral vortices on a rotating disk.

Jets in cross flow are important in several applications, such as film cooling of turbine blades. Key parameter of this flow is the *injection ratio R*, which is the ratio between the jet momentum flux and the free stream one. The very complex heat flux pattern over the surface a jet in cross flow is issuing from is shown in Fig. 5 where, again, the *heated-thin-foil* technique is used. Jet issues from a pipe (internal diameter D = 24 *mm*) has a Reynolds number Re = 8000 and exhausts in an aspirated subsonic wind tunnel. To reach the same temperature of free stream air so as to achieve two equal density flows, the jet air goes through a heat exchanger. The thermal map of Fig. 5, over the surface the jet is issuing from, shows the normalized Nusselt number *Nu/Nu0*, where *Nu0* is the Nusselt number measured with the pipe plugged (no jet), for injection ratio R = 3. Flow is again from left to right. The dashed and dotted circle indicates the pipe exit section and the white area refers to a region where no results are shown because there is either no heating (pipe exit), or data in these zones are affected by relevant edge effects (due to the high tangential conduction).

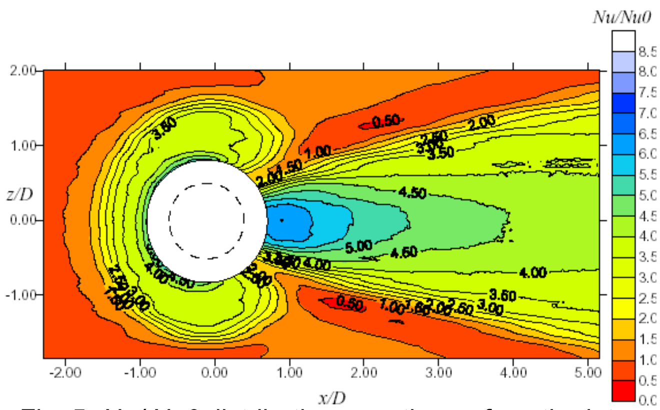

Fig. 5. *Nu/ Nu0* distribution over the surface the jet is issuing from, for R = 3 and Re = 8000.

There is no horseshoe vortex around the jet because of the high Reynolds number. The entrainment of the wall boundary layer gives ahead a strong increase of the heat transfer that tends to wrap around the pipe. At about *x/D* = 1, on the centerline, a maximum value of *Nu/Nu0* is evident which, for increasing *R*, weakens and moves slightly downstream. Starting at about *x/D* = 1 and *z/D* = ±1 and elongating downstream, two low heat transfer zones develop, where the convective heat transfer coefficient may attain values which are even below those measured without jet injection. This is due to a kind of free stream separation that is induced by the high momentum of the issuing jet which acts as an obstacle to the free stream. Results well agree with the findings of Carlomagno et al. (2004).

4. Conclusions

The use of infrared thermography as a powerful optical method to measure convective heat transfer coefficients in complex fluid flows is analyzed. Heat flux sensors usually used to measure convective heat transfer coefficients and exploitation of IRSR as a temperature measuring device are critically reviewed. The sensors different operating methods, together with the necessary implementations, are discussed in details for the *thin-film*, the *wall calorimeter* (transient techniques) and the *heated-thin-foil* (steady technique), sensors. Finally, several application are presented,

References

Astarita, T., Some Heat Transfer Aspects in Gas Turbines (in Italian), PhD Thesis. University of Naples (1996).

Astarita, T., Cardone, G. and Carlomagno, G. M., Spiral Vortices Detection on a Rotating Disk, CD-Rom Proc. 23rd Cong. Int. Council Aeronautical Sciences (Toronto), (2002), ICAS2002-3.6.4.

Carlomagno, G. M., Thermo-Fluid-Dynamics Applications of Quantitative Infrared Thermography, J. Flow Visualization Image Processing, 4 (1997), 261-280.

Carlomagno, G. M. and de Luca, L., Infrared Thermography in Convective Heat Transfer, in Handbook of Flow Visualization, Yang, W. J. ed., (2001), 547-575, Taylor & Francis, New York,.

Carlomagno, G. M., Nese, F. G., Cardone, G. and Astarita, T., Thermo-fluid-dynamics of a complex fluid flow, Infrared Physics Technology, 46 (2004), 31-39.

Cook, W. J. and Felderman, E. J., Reduction of Data from Thin-Film Heat-Transfer Gages: A Concise Numerical Technique, AIAA J., 4 (1966), 561-562.

De Luca, L., Cardone, G., Aymer de la Chevalerie, D. and Fonteneau, A., Experimental Analysis of Viscous Interaction in Hypersonic Wedge Flow, AIAA J., 33 (1995), 2293-2298.

Kakac, S., Shah, R. K. and Aung, W., Handbook of Single Phase Flow Convective Heat Transfer, (1987), Wiley, New York,.

Meola, C., de Luca, L. and Carlomagno, G. M., Influence of Shear Layer Dynamics on Impingement Heat Transfer, Experimental Thermal and Fluid Science, 13 (1996), 29-37.

Thompson, W. P., Heat Transfer Gages, in Methods of Experimental Physics, L. Marton and C. Marton ed., 18B (1981), 663-685, Academic Press, New York.

Author Profile

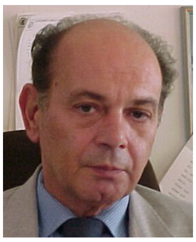

Giovanni Maria Carlomagno: He became Doctor in Mechanical Engineering (summa cum laude) in1965, Research assistant at Princeton University (1967-68), Associate professor of Physics (1969), Associate professor of Gas dynamics (1975), Professor of Aerospace and Mechanical Engineering (1986). He chaired over 20 International Meetings, is an editor of more than 20 books and an author of some 300 papers. He is a Member of the Scientific Council of the International Centre of Heat and Mass Transfer, of the Advisory Board of the Pacific Center of Thermal-Fluids Engineering, of the Executive Committee of the International Council for Aeronautical Sciences and of the Editorial Board of more than 10 Scientific International Journals, Chairman of the Technical Advisory Committee of the von Karman Institute and Dean of the Aerospace Engineering School at the University of Naples. Federico II.